Appl. Math. Mech. -Engl. Ed., **34**(11), 1327–1338 (2013)
DOI 10.1007/s10483-013-1748-7

Applied Mathematics and Mechanics (English Edition)

Non-uniform slot suction/injection into mixed convection boundary layer flow over vertical cone*

R. RAVINDRAN, M. GANAPATHIRAO

(Department of Mathematics, National Institute of Technology, Tiruchirappalli 620015, Tamilnadu, India)

Abstract The aim of this work is to study the effect of non-uniform single and double slot suction/injection into a steady mixed convection boundary layer flow over a vertical cone, while the axis of the cone is inline with the flow. The governing boundary layer equations are transformed into a non-dimensional form by a group of non-similar transformations. The resulting coupled non-linear partial differential equations are solved numerically by employing the quasi-linearization technique and an implicit finite-difference scheme. Numerical computations are performed for different values of the dimensionless parameters to display the velocity and temperature profiles graphically. Also, numerical results are presented for the skin friction and heat transfer coefficients. Results indicate that the skin friction and heat transfer coefficients increase with non-uniform slot suction, but the effect of non-uniform slot injection is just opposite.

Key words mixed convection, surface mass transfer, non-uniform slot suction, single and double slot, vertical cone

Chinese Library Classification O35
2010 Mathematics Subject Classification 76D05, 76M20, 35Q30, 35Q35

1 Introduction

The combination of free and forced convection is called the mixed convection. Mixed convection flow arises in many transport processes both natural and engineering applications. Convective heat transfer flow over a stationary cone is important for the thermal design of various types of industrial equipments such as stationary heat exchangers, design of canisters for nuclear waste disposal, nuclear reactor cooling system, and geothermal reservoirs. Moreover, heat transfer problems of mixed convection boundary layer flow over cones are extensively used by automobile and chemical industries.

Hering and Grosh[1] analyzed the practical case of mixed convection from a vertical rotating cone for the Prandtl number $Pr = 0.7$. Later, Himasekhar et al.[2] studied the combined convection flow over a vertical rotating cone for a wide range of Prandtl numbers. Mixed convection flow over a stationary and rotating vertical cylinders was studied in detail, by Mahmood and Merkin[3], Pop et al.[4], and Daskalakis[5]. Kumari et al.[6] and Yih[7] examined the heat transfer characteristics in mixed convection flow over a vertical cone without and with a porous media, respectively. Further, the mixed convection flow along a vertical cone of constant wall temperature was made by Pop et al.[8]. Recently, Ravindran et al.[9] obtained the non-similar

* Received Nov. 5, 2012 / Revised Jun. 3, 2013
Corresponding author R. RAVINDRAN, Ph. D., E-mail: ravir@nitt.edu

solution to examine the effect of uniform mass transfer on a steady mixed convection flow over a vertical cone.

Mass transfer from a wall slot into the boundary layer is of interest for various prospective applications, including thermal protection, energizing the inner portion of the boundary layers in adverse pressure gradients and skin friction reduction on high speed aircrafts. The finite discontinuities arise at the leading and trailing edges of the uniform slot suction/injection, and those can be removed by choosing appropriate non-uniform slot suction/injection, which was discussed by Minkowycz et al.[10].

Different studies were reported the influence of non-uniform single slot on a steady incompressible boundary layer flow over (i) a cylinder and (ii) a sphere[11], rotating sphere[12], yawed cylinder[13] and slender cylinder[14], respectively. Later, Roy and Saikrishnan[15] presented multiple slot in a diverging channel with exponentially decreasing free stream flow. Further, some investigators[16–18] studied the effect of non-uniform double slot into a steady incompressible flow over a slender cylinder, sphere, and cylinder, respectively.

Since no attempt has been made to study the effect of non-uniform single and double slot suction/injection into a steady mixed convection incompressible boundary layer flow over a vertical cone, we investigate this in the present study. Cone shaped bodies are often encountered in many engineering applications and many heat transfer problems of mixed convection flow. Moreover, heat transfer problems of mixed convection boundary layer flow over a stationary cone are extensively used by auto-mobile and chemical industries. Non-similar solutions are obtained numerically by solving coupled non-linear partial differential equations using the quasi-linearization technique and an implicit finite-difference scheme. Numerical results are obtained for different values of the Prandtl number, buoyancy, and suction/injection parameter. Some particular cases of the present results are compared with Kumari et al.[6], which indicates an excellent agreement.

2 Mathematical formulation

Consider the steady mixed convection laminar boundary layer flow of a viscous and incompressible fluid over a vertical cone with a half angle γ. It is assumed that the forced flow moves parallel to the axis of the cone in the upward direction with the free stream velocity u_∞ and uniform temperature of the ambient fluid T_∞. The uniform wall temperature of the cone T_w is higher than T_∞. The x-axis is taken along the surface of the cone measured from the apex, and the y-axis is normal to it, respectively. The physical model and coordinate system are shown in Fig. 1. Here, we assume that all the flow properties are constant except the density variation in the buoyancy force term. The buoyancy force arises due to the temperature differences in the fluid. Under these assumptions along with the Boussinesq approximation[19], the equations of conservation of mass, momentum, and energy governing the flow are listed as follows[20–21]:

$$\frac{\partial u}{\partial x} + \frac{\partial v}{\partial y} = 0, \tag{1}$$

$$u\frac{\partial u}{\partial x} + v\frac{\partial u}{\partial y} = u_\mathrm{e}\frac{\partial u_\mathrm{e}}{\partial x} + \nu\frac{\partial^2 u}{\partial y^2} + g\beta(T - T_\infty)\cos\gamma, \tag{2}$$

$$u\frac{\partial T}{\partial x} + v\frac{\partial T}{\partial y} = \frac{\nu}{Pr}\frac{\partial^2 T}{\partial y^2}, \tag{3}$$

where u and v are the velocity components along the x- and y-directions, respectively, g is the gravitational acceleration, β is the coefficient of thermal expansion, T is the temperature, ν is the kinematic viscosity, and Pr is the Prandtl number.

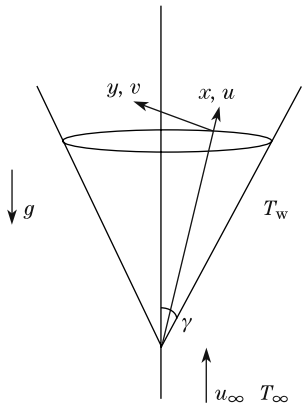

Fig. 1 Physical model and coordinate system

The boundary conditions adequate to the problem are given by

$$\begin{cases} u(x,0)=0, \quad v(x,0)=v_{\rm w}(x), \quad T(x,0)=T_{\rm w}=\text{constant}, \\ u(x,\infty)=u_{\rm e}=U(x)=u_\infty x^m, \quad T(x,\infty)=T_\infty=\text{constant}. \end{cases} \tag{4}$$

Here, the subscripts w and ∞ denote the conditions at the wall and infinity, respectively. The free stream velocity component is given by $U(x)=u_\infty x^m$, m is the exponent in the power law variation of the free stream velocity, and the exponent m is related to cone half angle γ by

$$\gamma=\frac{\pi m}{m+1} \quad \text{or} \quad m=\frac{\gamma}{\pi-\gamma}.$$

The external solution is given by $u_{\rm e}=U(x)=u_\infty x^m$ which is related to the exponent m by

$$m=\frac{x}{u_{\rm e}}\frac{{\rm d}u_{\rm e}}{{\rm d}x} \quad \text{or} \quad \frac{x}{U}\frac{{\rm d}U}{{\rm d}x}.$$

Hence, the external solution $u_{\rm e}$ is related to the cone half-angle γ by

$$\frac{\gamma}{\pi-\gamma} \;=\; \frac{x}{u_{\rm e}}\frac{{\rm d}u_{\rm e}}{{\rm d}x} \quad \text{or} \quad \frac{x}{U}\frac{{\rm d}U}{{\rm d}x}.$$

The following transformations reduce the system of partial differential equations (1)–(3) to a non-dimensional form:

$$\begin{cases} \xi=\Big(\dfrac{2}{m+1}\dfrac{\nu x}{U}\Big)^{\frac{1}{2}}, \quad \eta=y\Big(\dfrac{m+1}{2}\dfrac{U}{\nu x}\Big)^{\frac{1}{2}}, \\ \psi(x,y)=\Big(\dfrac{2}{m+1}\nu x U\Big)^{\frac{1}{2}}f(\xi,\eta), \quad u=\dfrac{\partial\psi}{\partial y}, \quad v=-\dfrac{\partial\psi}{\partial x}, \\ f_\eta(\xi,\eta)=F(\xi,\eta), \quad u=UF(\xi,\eta), \quad G(\xi,\eta)=\dfrac{T-T_\infty}{T_{\rm w}-T_\infty}, \\ v=-2^{-1}\Big(\dfrac{2}{m+1}\dfrac{\nu U}{x}\Big)^{\frac{1}{2}}((m+1)f+(1-m)(\xi f_\xi-\eta F)). \end{cases} \tag{5}$$

Here, ξ and η are the transformed coordinates, ψ and f are the dimensional and dimensionless stream functions, respectively, and F and G are the dimensionless velocity and temperature, respectively.

Equation (1) is automatically satisfied, and Eqs. (2) and (3) after transformation take the follwing forms:

$$F_{\eta\eta} + fF_\eta + \frac{2m}{m+1}(1-F^2) + \frac{2}{m+1}\lambda G = \Big(\frac{1-m}{m+1}\Big)\xi(FF_\xi - F_\eta f_\xi), \tag{6}$$

$$Pr^{-1}G_{\eta\eta} + fG_\eta = \Big(\frac{1-m}{m+1}\Big)\xi(FG_\xi - G_\eta f_\xi), \tag{7}$$

where

$$Pr = \frac{\mu c_p}{k}, \quad Gr_x = \frac{g\beta x^3(T_\mathrm{w} - T_\infty)\cos\gamma}{\nu^2}, \quad Re_x = \frac{Ux}{\nu}, \quad \lambda = \frac{Gr_x}{Re_x^2}.$$

Here, the subscripts ξ and η denote the partial derivatives with respect to these variables, μ is the dynamic viscosity, c_p is the specific heat at constant pressure, k is the thermal conductivity, Gr_x is the local Grashof number, Re_x is the Reynolds number, and λ is the buoyancy parameter.

The transformed boundary conditions are

$$\begin{cases} F(\xi,0) = 0, \quad G(\xi,0) = 1 \quad \text{at} \quad \eta = 0, \\ F(\xi,\eta_\infty) = 1, \quad G(\xi,\eta_\infty) = 0 \quad \text{at} \quad \eta = \eta_\infty, \end{cases} \tag{8}$$

where $f = \displaystyle\int_0^\eta F\mathrm{d}\eta + f_\mathrm{w}$, and f_w is given by

$$f_\mathrm{w} + \Big(\frac{1-m}{m+1}\Big)\xi(f_\xi)_\mathrm{w} = -\Big(\frac{v_\mathrm{w}}{\nu}\Big)\xi.$$

From the above equation, one can easily obtain

$$f_\mathrm{w} = \frac{-1}{\nu}\Big(\frac{1+m}{1-m}\Big)\xi^{-\frac{1+m}{1-m}}\int_0^\xi v_\mathrm{w}(\xi)\xi^{\frac{1+m}{1-m}}\mathrm{d}\xi.$$

Equations (6) and (7) with boundary conditions (8) can be solved numerically. In particular, here we study the effect of non-uniform single and double slot suction/injection into boundary layer flow over a vertical cone in subsections sections 2.1 and 2.2, respectively.

2.1 Single slot

In the case of single slot, the value f_w is given by

$$f_\mathrm{w} = \begin{cases} 0, \quad \xi \leqslant \xi_0, \\ A\xi^{-\frac{1+m}{1-m}}C(\xi,\xi_0), \quad \xi_0 \leqslant \xi \leqslant \xi_0^*, \\ A\xi^{-\frac{1+m}{1-m}}C(\xi_0^*,\xi_0), \quad \xi \geqslant \xi_0^*, \end{cases} \tag{9}$$

where the function

$$C(\xi,\xi_0) = 1 - \cos(\omega^*(\xi - \xi_0)).$$

Here, $v_\mathrm{w}(\xi)$ is taken as

$$v_\mathrm{w}(\xi) = \begin{cases} 0, \quad \xi \leqslant \xi_0, \\ -\nu\Big(\frac{1-m}{1+m}\Big)A\xi^{-\frac{1+m}{1-m}}\omega^*\sin(\omega^*(\xi - \xi_0)), \quad \xi_0 \leqslant \xi \leqslant \xi_0^*, \\ 0, \quad \xi \geqslant \xi_0^*, \end{cases}$$

where ω^* is the slot length, and ξ_0 is the starting point of slot position. The function $v_{\rm w}(\xi)$ is continuous for all the values of ξ, and it has a non-zero value only in the interval $[\xi_0, \xi_0^*]$. This type of function allows the mass transfer to change slowly in the neighbourhood of the leading and trailing edges of the slot. The mass transfer parameter $A > 0$ or $A < 0$ indicates the suction or injection, respectively.

2.2 Double slot

In the case of double slot, the value $f_{\rm w}$ is given by

$$f_{\rm w} = \begin{cases} 0, \quad \xi \leqslant \xi_0, \\ A\xi^{-\frac{1+m}{1-m}} C(\xi, \xi_0), \quad \xi_0 \leqslant \xi \leqslant \xi_0^*, \\ A\xi^{-\frac{1+m}{1-m}} C(\xi_0^*, \xi_0), \quad \xi_0^* \leqslant \xi \leqslant \xi_1, \\ A\xi^{-\frac{1+m}{1-m}} C(\xi_0^*, \xi_0) + A\xi^{-\frac{1+m}{1-m}} C(\xi, \xi_1), \quad \xi_1 \leqslant \xi \leqslant \xi_1^*, \\ A\xi^{-\frac{1+m}{1-m}} C(\xi_0^*, \xi_0) + A\xi^{-\frac{1+m}{1-m}} C(\xi_1^*, \xi_1), \quad \xi \geqslant \xi_1^*. \end{cases} \tag{10}$$

Here, $v_{\rm w}(\xi)$ is taken as

$$v_{\rm w}(\xi) = \begin{cases} 0, \quad \xi \leqslant \xi_0, \\ -\nu\Big(\dfrac{1-m}{1+m}\Big) A\xi^{-\frac{1+m}{1-m}} \omega^* \sin(\omega^*(\xi - \xi_0)), \quad \xi_0 \leqslant \xi \leqslant \xi_0^*, \\ 0, \quad \xi_0^* \leqslant \xi \leqslant \xi_1, \\ -\nu\Big(\dfrac{1-m}{1+m}\Big) A\xi^{-\frac{1+m}{1-m}} \omega^* \sin(\omega^*(\xi - \xi_1)), \quad \xi_1 \leqslant \xi \leqslant \xi_1^*, \\ 0, \quad \xi \geqslant \xi_1^*, \end{cases}$$

where ω^* is the slot length, and ξ_0 and ξ_1 are the two free parameters which determine the starting points of the first and second slot positions, respectively. Hence, the continuous function $v_{\rm w}(\xi)$ has a non-zero value only in the intervals $[\xi_0, \xi_0^*]$ and $[\xi_1, \xi_1^*]$.

It may be remarked that the Eqs. (6) and (7) with $\xi = 0$, $\lambda = 0$, $m = 0$, and $A = 0$ coincide with those of Kumari et al.[6].

The important physical quantities are given by the skin friction coefficient

$$C_{\rm f} = \frac{2\big(\mu\big(\frac{\partial u}{\partial y}\big)\big)_{\rm w}}{\rho U^2} = 2(Re_x)^{-\frac{1}{2}} \Big(\frac{m+1}{2}\Big)^{\frac{1}{2}} (F_\eta)_{\rm w}$$

and the heat transfer coefficient in terms of the Nusselt number

$$Nu = -\frac{\big(x\big(\frac{\partial T}{\partial y}\big)\big)_{\rm w}}{(T_{\rm w} - T_\infty)} = -(Re_x)^{\frac{1}{2}} \Big(\frac{m+1}{2}\Big)^{\frac{1}{2}} (G_\eta)_{\rm w}.$$

Here, ρ is the density. Thus,

$$(Re_x)^{\frac{1}{2}} C_{\rm f} = 2\Big(\frac{m+1}{2}\Big)^{\frac{1}{2}} (F_\eta)_{\rm w}, \tag{11}$$

$$(Re_x)^{-\frac{1}{2}} Nu = -\Big(\frac{m+1}{2}\Big)^{\frac{1}{2}} (F_\eta)_{\rm w}. \tag{12}$$

3 Method of solution

The coupled non-linear partial differential equations (6) and (7) with boundary conditions (8) represent a two point boundary value problem for partial differential equations were solved numerically by employing an implicit finite-difference scheme in combination with the quasi-linearization technique[22–23].

Linearizing Eqs. (6) and (7) by using quasi-linearization technique, the following set of linear differential equations are obtained:

$$F_{\eta\eta}^{i+1} + X_1^i F_\eta^{i+1} + X_2^i F^{i+1} + X_3^i F_\xi^{i+1} + X_4^i G^{i+1} = X_5^i, \tag{13}$$

$$G_{\eta\eta}^{i+1} + Y_1^i G_\eta^{i+1} + Y_2^i G_\xi^{i+1} + Y_3^i F^{i+1} = Y_4^i. \tag{14}$$

The coefficient functions with iterative index i are known, and the functions with iterative index $(i+1)$ are to be determined.

The boundary conditions (8) become

$$\begin{cases} F^{i+1} = 0, \quad G^{i+1} = 1 \quad \text{at} \quad \eta = 0, \\ F^{i+1} = 1, \quad G^{i+1} = 0 \quad \text{at} \quad \eta = \eta_\infty, \end{cases} \tag{15}$$

where η_∞ is the edge of the boundary layer.

The coefficients in Eqs. (13) and (14) are as follows:

$$X_1^i = f + \Big(\frac{1-m}{m+1}\Big)\xi f_\xi,$$

$$X_2^i = -\Big(\frac{4m}{m+1}\Big)F - \Big(\frac{1-m}{m+1}\Big)\xi F_\xi,$$

$$X_3^i = -\Big(\frac{1-m}{m+1}\Big)\xi F,$$

$$X_4^i = \Big(\frac{2}{m+1}\Big)\lambda,$$

$$X_5^i = -\Big(\frac{2m}{m+1}\Big)(1+F^2) - \Big(\frac{1-m}{m+1}\Big)\xi F F_\xi,$$

$$Y_1^i = Pr\Big(f + \Big(\frac{1-m}{m+1}\Big)\xi f_\xi\Big),$$

$$Y_2^i = -Pr\Big(\frac{1-m}{m+1}\Big)\xi F,$$

$$Y_3^i = -Pr\Big(\frac{1-m}{m+1}\Big)\xi G_\xi,$$

$$Y_4^i = -Pr\Big(\frac{1-m}{m+1}\Big)\xi F G_\xi.$$

The finite-difference scheme is applied to Eqs. (13) and (14). Central difference formulae are used in the η-direction and the backward difference formulae in the stream-wise direction ξ with constant step sizes $\Delta\eta$ and $\Delta\xi$ in the η- and ξ-directions, respectively. The resulting system of linear algebraic equations with a block tri-diagonal matrix which is solved by using Varga's algorithm[24].

The step sizes in the η- and ξ-directions are chosen as $\Delta\eta = 0.05$ and $\Delta\xi = 0.01$, respectively. A convergence criterion based on the relative difference between the current and previous iterations is used. The iteration procedure is continued until the convergence criterion $\max(|(F_\eta)_{\mathrm{w}}^{i+1} - (F_\eta)_{\mathrm{w}}^{i}|, |(G_\eta)_{\mathrm{w}}^{i+1} - (G_\eta)_{\mathrm{w}}^{i}|) < 10^{-4}$ is satisfied.

4 Results and discussion

In order to validate the accuracy of our numerical method, solutions are obtained for $\xi = 0$, $\lambda = 0$, $m = 0$, and $A = 0$ to compare the velocity and temperature profiles (F and G) with those of Kumari et al.[6] for different values of the Prandtl number, $Pr = 0.733$ and 6.7. The results are found to be in good agreement, and the comparison is shown in Fig. 2. Computations are carried out for various values of $Pr\,(0.7 \leqslant Pr \leqslant 7.0)$, $A\,(-0.5 \leqslant A \leqslant 0.5)$, and $\lambda\,(-1.605 \leqslant \lambda \leqslant 5)$. In all numerical computations, m is taken as 0.5, and the edge of the boundary layer η_∞ is taken as 7.0.

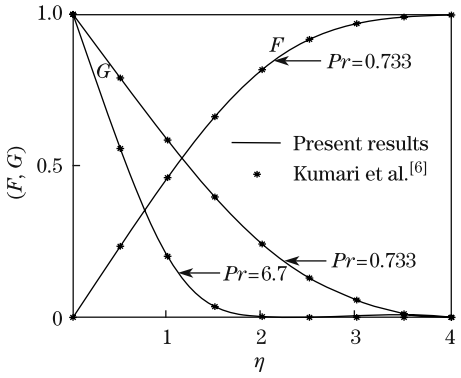

Fig. 2 Comparison of velocity and temperature profiles with those of Kumari et al.[6] when $\xi = 0$, $\lambda = 0$, $m = 0$, and $A = 0$

The effects of the buoyancy parameter λ and the Prandtl number Pr on velocity and temperature profiles (F, G) for $m = 0.5$, $A = 0.5$, and $\omega^* = \pi$ are shown in Figs. 3 and 4. Both buoyancy assisting ($\lambda > 0$) and opposing ($\lambda < 0$) forces are considered. It is observed from Fig. 3 that the buoyancy assisting flow shows the overshoot in the velocity profiles near the wall for lower Prandtl number fluid ($Pr = 0.7$, air), but for higher Prandtl number fluid ($Pr = 7.0$, water), the velocity overshoot is not observed. The magnitude of the overshoot increases with $\lambda\,(\lambda > 0)$. The physical reason is that the buoyancy force λ effect is larger in a lower Prandtl number fluid ($Pr = 0.7$, air) due to low viscosity of the fluid, which enhances the velocity within the boundary layer as the assisting buoyancy force acts like a favorable pressure gradient, and the velocity overshoot occurs. For higher values of $Pr\,(Pr = 7.0$, water), the velocity overshoot is not observed because the higher Prandtl number fluid means more viscous fluid which has less impact on the buoyancy parameter. Higher Prandtl number ($Pr = 0.7$, air) fluid has a lower thermal conductivity in a thinner thermal boundary layer as shown in Fig. 4.

The effects of the surface mass transfer parameter A and buoyancy parameter λ on velocity and temperature profiles (F, G) for $Pr = 0.7$, $m = 0.5$, $\omega^* = \pi$, and $\xi = 1.0$ are shown in Figs. 5 and 6. It is observed from Fig. 5, for buoyancy assisting force ($\lambda > 0$), the velocity overshoot is observed for injection ($A < 0$), and the overshoot reduced by suction ($A > 0$), and for buoyancy opposing force ($\lambda < 0$), the reverse flow starts at $\lambda = -0.96$ for $Pr = 0.7$ and at $\lambda = -1.6$ for $Pr = 7.0$ when $A = 0$. The buoyancy opposing force acts as an adverse pressure gradient which reduces the velocity near the wall within the boundary layer. Subsequently further decreases in the value of λ, the fluid flow backward within small region near the wall creating a back flow region attached to wall can be seen in Fig. 5. It is noticed in Fig. 5, for buoyancy opposing force, there is no reverse flow occurs when $A = 0.5$. This gives an idea to control the reverse flow for negative values of buoyancy parameter through non-uniform slot suction. The physical reason is that the lower energy fluid near the wall removes from the boundary layer through non-uniform slot suction. Figure 6 shows that the thickness of the temperature boundary layer

decreases by increasing of suction as the well as buoyancy force ($\lambda > 0$).

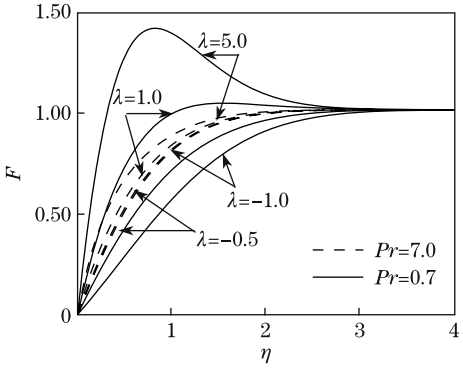

Fig. 3 Effect of λ and Pr on velocity profiles at $\xi = 1.0$ when $m = 0.5$, $A = 0.5$, and $\omega^* = \pi$

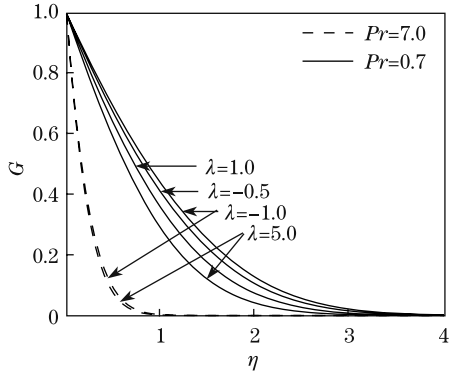

Fig. 4 Effect of λ and Pr on temperature profiles at $\xi = 1.0$ when $m = 0.5$, $A = 0.5$, and $\omega^* = \pi$

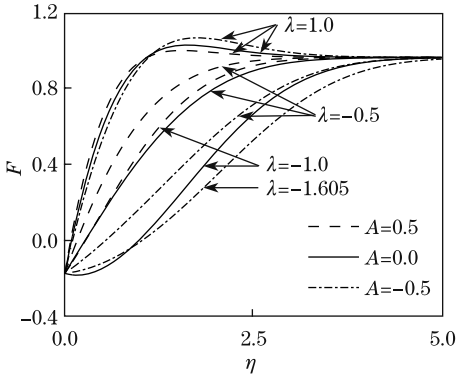

Fig. 5 Effect of non-uniform slot suction and injection on velocity profiles at $\xi = 1.0$ when $Pr = 0.7$, $m = 0.5$, and $\omega^* = \pi$ at slot position $[\xi_0 = 0.5, \xi_0^* = 1.0]$

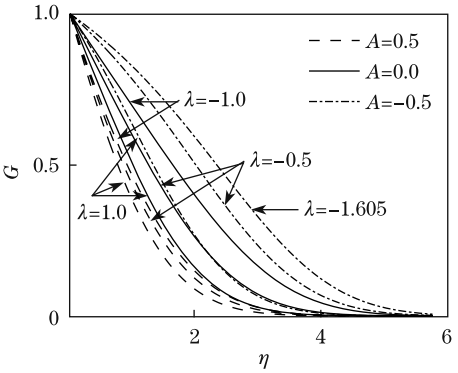

Fig. 6 Effect of non-uniform slot suction and injection on temperature profiles at $\xi = 1.0$ when $Pr = 0.7$, $m = 0.5$, and $\omega^* = \pi$ at slot position $[\xi_0 = 0.5, \xi_0^* = 1.0]$

Figures 7 and 8 display the effect of non-uniform singe slot suction ($A > 0$) and injection ($A < 0$) on skin friction and heat transfer coefficients ($C_{\mathrm{f}}(Re_x)^{\frac{1}{2}}$, $Nu(Re_x)^{\frac{-1}{2}}$) for $\lambda = 1.0$, $Pr = 0.7$, $m = 0.5$, $\omega^* = 2\pi$, and $\xi_0 = 0.5$. In the case of non-uniform slot suction, the skin friction and heat transfer coefficients increase as the slot starts and attain their maximum values before the trailing edge of the slot. Finally, $C_{\mathrm{f}}(Re_x)^{\frac{1}{2}}$ and $Nu(Re_x)^{\frac{-1}{2}}$ decrease from their maximum values and reach a finite value. Non-uniform slot injection has the reverse effect. It can be observed from Fig. 7, the upstream velocity gradient effect carries over beyond the location at $\xi = 1.0$, displaying the slight oscillation in skin friction profile but there is no oscillation in heat transfer profiles as observed in Fig. 8. Suction thins the boundary layer and greatly increases the wall slope (skin friction and heat transfer), but injection thickens the boundary layer and reduces the skin friction and heat transfer coefficients. As an increase in suction parameter, skin friction and heat transfer coefficients increase, while they decrease by increasing of injection. In particular, for $\lambda = 1.0$, $Pr = 0.7$, and $\xi = 0.75$, the increase of suction parameter from $A = 0.2$ to $A = 0.5$ results in increase of $C_{\mathrm{f}}(Re_x)^{\frac{1}{2}}$ and $Nu(Re_x)^{\frac{-1}{2}}$ are approximately 34% and 73.6%, respectively. On the other hand, $C_{\mathrm{f}}(Re_x)^{\frac{1}{2}}$ and $Nu(Re_x)^{\frac{-1}{2}}$

are decreased approximately 33% and 74%, respectively, by increasing the injection parameter from $A = -0.2$ to $A = -0.5$.

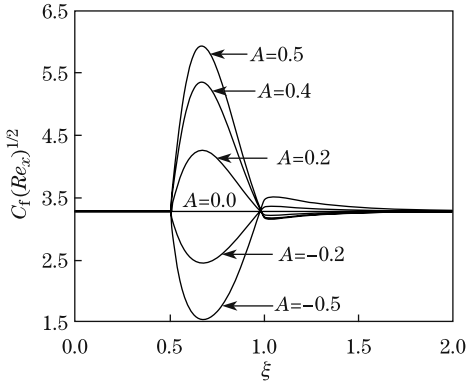

Fig. 7 Effect of non-uniform single slot suction and injection on $C_f(Re_x)^{\frac{1}{2}}$ when $\lambda = 1.0$, $Pr = 0.7$, $m = 0.5$, and $\omega^* = 2\pi$ at slot position $[\xi_0 = 0.5, \xi_0^* = 1.0]$

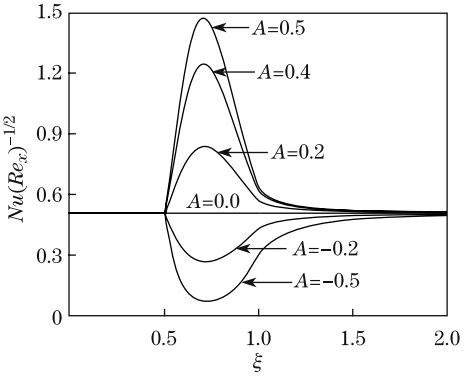

Fig. 8 Effect of non-uniform single slot suction and injection on $Nu(Re_x)^{\frac{-1}{2}}$ when $\lambda = 1.0$, $Pr = 0.7$, $m = 0.5$, and $\omega^* = 2\pi$ at slot position $[\xi_0 = 0.5, \xi_0^* = 1.0]$

The downstream movements of the single slot suction/injection at different stream-wise locations $[\xi_0 = 0.5, \xi_0^* = 1.0]$ and $[\xi_0 = 0.75, \xi_0^* = 1.25]$ on skin friction and heat transfer coefficients $(C_f(Re_x)^{\frac{1}{2}}, Nu(Re_x)^{\frac{-1}{2}})$ are shown in Figs. 9 and 10, when $\lambda = 1.0$, $Pr = 0.7$, $m = 0.5$, and $\omega^* = 2\pi$. It is observed that, if we move the location of the slot downstream, the skin friction and heat transfer coefficients decrease by suction. Non-uniform slot injection is just opposite. In specific, when $\lambda = 1.0$, $Pr = 0.7$, and $A = 0.5$, results in decrease of $C_f(Re_x)^{\frac{1}{2}}$ and $Nu(Re_x)^{\frac{-1}{2}}$ are approximately 18% and 34%, respectively, at the middle of the slots.

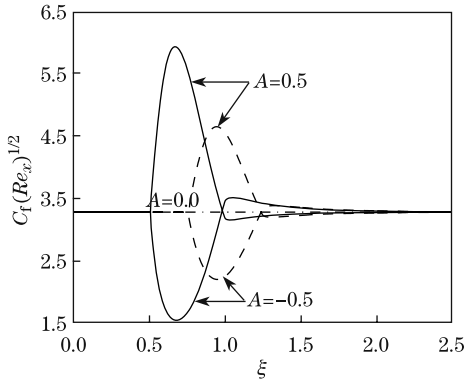

Fig. 9 Effect of downstream movement of non-uniform single slot suction and injection on $C_f(Re_x)^{\frac{1}{2}}$ when $\lambda = 1.0$, $Pr = 0.7$, $m = 0.5$, and $\omega^* = 2\pi$ at slot positions $[\xi_0 = 0.5, \xi_0^* = 1.0]$ and $[\xi_0 = 0.75, \xi_0^* = 1.25]$

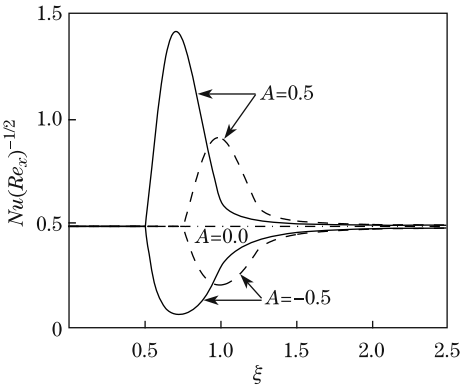

Fig. 10 Effect of downstream movement of non-uniform single slot suction and injection on $Nu(Re_x)^{\frac{-1}{2}}$ when $\lambda = 1.0$, $Pr = 0.7$, $m = 0.5$, and $\omega^* = 2\pi$ at slot positions $[\xi_0 = 0.5, \xi_0^* = 1.0]$ and $[\xi_0 = 0.75, \xi_0^* = 1.25]$

The effects of non-uniform double slot suction/injection on skin friction and heat transfer coefficients $(C_f(Re_x)^{\frac{1}{2}}, Nu(Re_x)^{\frac{-1}{2}})$ for $\lambda = 1.0$, $Pr = 0.7$, $m = 0.5$, and $\omega^* = 2\pi$ are shown in Figs. 11 and 12. In the case of double slot suction, the skin friction and heat transfer

coefficients increase as the first slot begins and attain their maximum values before the trailing edge of the first slot. Next, $C_{\mathrm{f}}(Re_x)^{\frac{1}{2}}$ and $Nu(Re_x)^{\frac{-1}{2}}$ decrease their maximum values at the trailing edge of the first slot. Similar variations on $C_{\mathrm{f}}(Re_x)^{\frac{1}{2}}$ and $Nu(Re_x)^{\frac{-1}{2}}$ are found in the second slot. It is observed that the effect slot suction on $C_{\mathrm{f}}(Re_x)^{\frac{1}{2}}$ and $Nu(Re_x)^{\frac{-1}{2}}$ is less in the second slot when compared with the first slot. Non-uniform double slot injection is just opposite. In specific, for $\lambda = 1.0$, $Pr = 0.7$ due to the increase of suction parameter from 0.25 to 0.5, the percentages of increase in $C_{\mathrm{f}}(Re_x)^{\frac{1}{2}}$ and $Nu(Re_x)^{\frac{-1}{2}}$ are approximately 27% and 56%, respectively, at the middle of the first slot ($\xi = 0.75$) whereas the respective increase in $C_{\mathrm{f}}(Re_x)^{\frac{1}{2}}$ and $Nu(Re_x)^{\frac{-1}{2}}$ are approximately 5.6% and 10.2%, at the middle of the second slot ($\xi = 1.75$).

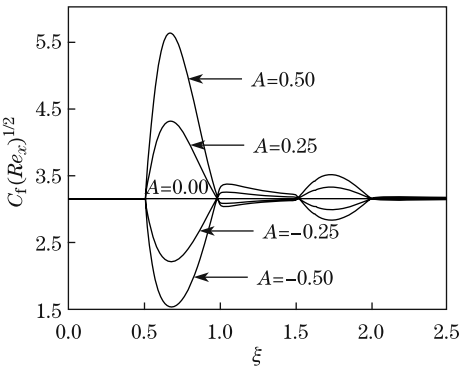

Fig. 11 Effect of non-uniform double slot suction and injection on $C_{\mathrm{f}}(Re_x)^{\frac{1}{2}}$ when $\lambda = 1.0$, $Pr = 0.7$, $m = 0.5$, and $\omega^* = 2\pi$ at slot positions $[\xi_0 = 0.5, \xi_0^* = 1.0]$ and $[\xi_1 = 1.5, \xi_1^* = 2.0]$

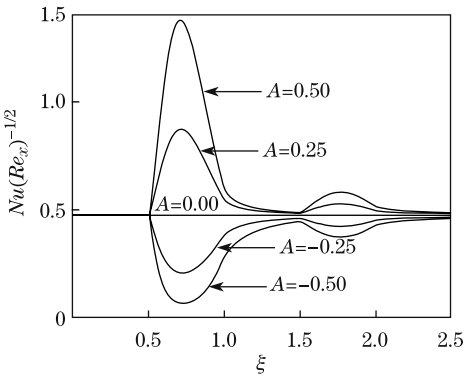

Fig. 12 Effect of non-uniform double slot suction and injection on $Nu(Re_x)^{\frac{-1}{2}}$ when $\lambda = 1.0$, $Pr = 0.7$, $m = 0.5$, and $\omega^* = 2\pi$ at slot positions $[\xi_0 = 0.5, \xi_0^* = 1.0]$ and $[\xi_1 = 1.5, \xi_1^* = 2.0]$

5 Conclusions

We obtain the non-similar solution of a steady mixed convection flow over a vertical cone through non-uniform single and double slot suction/injection. The main conclusions of this study are as follows:

(i) The buoyancy assisting flow to cause overshoot in the velocity profiles for lower Prandtl number fluids ($Pr = 0.7$, air) and the overshoot is not observed for higher Prandtl number fluids ($Pr = 7.0$, water).

(ii) Higher Prandtl number fluid ($Pr = 7.0$, water) causes a thinner thermal boundary layer.

(iii) The velocity and thermal boundary layer thicknesses are reduced by the increase of suction as well as the buoyancy parameter.

(iv) The increase of buoyancy parameter λ and injection parameter ($A < 0$) tend to increase the magnitude of the velocity overshoot, but the suction parameter ($A > 0$) reduces the magnitude of the velocity overshoot.

(v) Non-uniform slot suction helps to control the back flow for negative values of buoyancy parameter which confirms the importance of present study of the non-uniform slot.

(vi) Skin friction and heat transfer coefficients increase with the increase of mass transfer rates, i.e., the value of A ($A > 0$).

(vii) Non-uniform slot injection helps to reduce the skin friction and heat transfer coefficients at a particular stream-wise location on the cone surface.

(viii) When the slot moves along the downstream direction, the skin friction and heat transfer coefficients are decreased by suction, but it is opposite for injection.

Acknowledgements Authors express sincere thanks to the anonymous reviewers for their detailed and very useful comments in improving the quality of the manuscript. One of the authors (M. GANAPATHIRAO) is thankful to the Ministry of Human Resource Development, the Government of India for the grant of a fellowship to pursue this work.

References

[1] Hering, R. G. and Grosh, R. J. Laminar combined convection from a rotating cone. *ASME Journal of Heat Transfer*, **85**, 29–34 (1963)

[2] Himasekhar, K., Sarma, P. K., and Janardhan, K. Laminar mixed convection from a vertical rotating cone. *International Communications in Heat and Mass Transfer*, **16**, 99–106 (1989)

[3] Mahmood, T. and Merkin, J. H. Mixed convection on a vertical circular cylinder. *Journal of Applied Mathematics and Physics* (*ZAMP*), **39**, 186–203 (1988)

[4] Pop, I., Kumari, M., and Nath, G. Combined free and forced convection along a rotating vertical cylinder. *International Journal of Engineering Science*, **27**, 193–202 (1989)

[5] Daskalakis, J. E. Mixed free and forced convection in the incompressible boundary layer along a rotating vertical cylinder with fluid injection. *International Journal of Energy Research*, **17**, 689–695 (1993)

[6] Kumari, M., Pop, I., and Nath, G. Mixed convection along a vertical cone. *International Communications in Heat and Mass Transfer*, **16**, 247–255 (1989)

[7] Yih, K. A. Mixed convection about a cone in a porous medium: the entire regime. *International Communications in Heat and Mass Transfer*, **26**, 1041–1050 (1999)

[8] Pop, I., Grosan, T., and Kumari, M. Mixed convection along a vertical cone for fluids of any Prandtl number: case of constant wall temperature. *International Journal of Numerical Methods for Heat and Fluid Flow*, **13**, 815–829 (2003)

[9] Ravindran, R., Roy, S., and Momoniat, E. Effects of injection (suction) on a steady mixed convection boundary layer flow over a vertical cone. *International Journal of Numerical Methods for Heat and Fluid Flow*, **19**, 432–444 (2009)

[10] Minkowycz, W. J., Sparrow, E. M., Schneider, G. E., and Pletcher, R. H. *Handbook of Numerical Heat Transfer*, John Wiley & Sons, New York (1988)

[11] Saikrishnan, P. and Roy, S. Non-uniform slot injection (suction) into water boundary layers over (i) a cylinder and (ii) a sphere. *International Journal of Engineering Science*, **41**, 1351–1365 (2003)

[12] Roy, S. and Saikrishnan, P. Non-uniform slot injection (suction) into steady laminar water boundary layer flow over a rotating sphere. *International Journal of Heat and Mass Transfer*, **46**, 3389–3396 (2003)

[13] Roy, S. and Saikrishnan, P. Non-uniform slot injection (suction) into water boundary layer flow past yawed cylinder. *International Journal of Engineering Science*, **42**, 2147–2157 (2004)

[14] Datta, P., Anilkumar, D., Roy, S., and Mahanti, N. C. Effect of non-uniform slot injection (suction) on a forced flow over a slender cylinder. *International Journal of Heat and Mass Transfer*, **49**, 2366–2371 (2006)

[15] Roy, S. and Saikrishnan, P. Multiple slot suction/injection into an exponentially decreasing free stream flow. *International Communications in Heat and Mass Transfer*, **35**, 163–168 (2008)

[16] Roy, S., Datta, P., Ravindran, R., and Momoniat, E. Non-uniform double slot injection (suction) on a forced flow over a slender cylinder. *International Journal of Heat and Mass Transfer*, **50**, 3190–3194 (2007)

[17] Roy, S., Saikrishnan, P., and Bishun, D. P. Influence of double slot suction (injection) into water boundary layer flows over sphere. *International Communications in Heat and Mass Transfer*, **36**, 646–650 (2009)

[18] Saikrishnan, P., Roy, S., Mohammed, R. S., and Bishun, D. P. Non-uniform double slot suction (injection) into water boundary layer flows over a cylinder. *International Journal of Heat and Mass Transfer*, **52**, 894–898 (2009)

[19] Schlichting, H. and Gersten, K. *Boundary Layer Theory*, Springer, New York (2000)

[20] Bejan, A. *Convection Heat Transfer*, John Wiley & Sons, New York (2004)

[21] Pop, I. and Ingham, D. B. *Convective Heat Transfer*: *Mathematical and Computational Modelling of Viscous Fluids and Porous Media*, Pergamon, Oxford (2001)

[22] Singh, P. J. and Roy, S. Unsteady mixed convection flow over a vertical cone due to impulsive motion. *International Journal of Heat and Mass Transfer*, **50**, 949–959 (2007)

[23] Bellman, R. E. and Kalaba, R. E. *Quasilinearization and Non-linear Boundary-Value Problems*, American Elsevier Publishing Company Incorporation, New York (1965)

[24] Varga, R. S. *Matrix Iterative Analysis*, Springer, New York (2000)